applied sciences

MDPI

Article

Pitting Corrosion in AISI 304 Rolled Stainless Steel Welding at Different Deformation Levels

Francisco-Javier Cárcel-Carrasco [1], Manuel Pascual-Guillamón [1], Lorenzo Solano García [2,*], Fidel Salas Vicente [1] and Miguel-Angel Pérez-Puig [1]

1 ITM, Universitat Politècnica de València, 46022 Valencia, Spain
2 Departamento de Ingeniería Mecánica y de Materiales, Universitat Politècnica de València, 46022 Valencia, Spain
* Correspondence: lsolano@mcm.upv.es; Tel.: +34-963-87-7000 (ext. 76273); Fax: +34-963-87-7627

Received: 12 July 2019; Accepted: 7 August 2019; Published: 9 August 2019

Abstract: This paper analyzes pitting corrosion at the weld zone and at the heat affected zone (HAZ) in AISI 304 rolled stainless steel welds. As the aforementioned material is one of the most frequently used types of stainless steel, it is needful to be aware of the mechanisms that lead to its deterioration, like corrosion, since it can cause failures or malfunction in a wide variety of products and facilities. For the experimental tests 1.5 mm thick AISI 304 stainless steel plates were welded and rolled to different thicknesses and after, the samples were subjected to mechanical and corrosion tests and to a micrograph study. Deformation stresses and other intrinsic metallurgic and physic-chemical transformations that occur during cold rolling and welding, and that are key factors in the anti-corrosion behavior of AISI 304 rolled stainless steel, have been observed and analyzed. A correlation has been found between cold work levels in test samples and number of pits after corrosion tests.

Keywords: pitting corrosion; welding; cold rolling; deformation stress; AISI 304; AISI 308L

1. Introduction

The objective of this study is to analyze the resistance of AISI 304 welds to pitting corrosion when they have been subjected to different levels of cold rolling, as well as to establish a correlation between the pitting corrosion and cold rolling deformation level.

The pitting corrosion, initiated at certain points of the surface due to the non-uniformity of the passive layer, is a localized redox (reduction-oxidation) process that occurs inside small pits on the surface of passivated metals in aqueous media. This kind of reaction requires the balancing of both the reduction and oxidation half-reactions. The anodic reaction that takes place inside the pit leads to the dissolution of iron ($Fe \rightarrow Fe^{2+} + 2e^-$) while the cathodic reaction, that makes use of the electrons liberated by the anodic reaction, leads to the apparition of hydroxide ($1/2O_2 + H_2O + 2e^- \rightarrow 2(OH^-)$). As inside the pit, the electrolyte solution becomes positively charged due to the presence of Fe^{2+} ions, the anionic species (Cl^-) in the electrolyte are attracted there, increasing the acidity inside the pit and accelerating the corrosion process according to the reactions:

$$FeCl_3 \rightarrow Fe^{3+} + 3Cl^- \quad \text{(outside the pit)}$$
$$Fe^{3+} + 3(OH)^- \rightarrow Fe(OH)_3 \quad \text{(outside the pit)}$$
$$Fe^{2+} + 2Cl^- \rightarrow FeCl_2 \quad \text{(at the pit)}$$
$$FeCl_2 + 2H_2O \rightarrow Fe(OH)_2 + 2HCl \quad \text{(at the pit)}$$

Furthermore, the solid $Fe(OH)_3$ deposited around the pit increases the separation of the inside of the pit from the rest of the electrolyte. The presence of chemical species that provide a high concentration of Cl^- in the aqueous media is needed to accelerate the process of corrosion in the pit.

AISI 304 stainless steel is widely used in the manufacturing of both industrial and domestic products, mainly due to the combination of characteristics that presents: Good mechanical properties (high strength, ductility and malleability); non-magnetic behavior; weldability; resistance to corrosion and low cost [1–4]. It is used in applications that entail a high stress level and/or exposure to corrosive atmospheres, like in nuclear power plants [5,6], marine environments [7,8] or in large facilities [9]. Particularly, AISI 304 rolled stainless steel is one of the most frequently used types of stainless steel, whereby it is needful to be aware of the mechanisms that lead to its deterioration in order to foresee, restrict and/or quantify the economic costs that could be derived. Corrosion is one of the key factors to consider, as it can cause failures or malfunction in all types of products and facilities. Specially, when they get in contact with corrosive agents or when they are used in conditions or participate in processes that bring on corrosion [8], like welding and cold forming.

The anti-corrosion behavior of welded stainless steels has been studied previously [10]. AISI 304 stainless steel can be welded by almost all the common welding techniques [11]. In arc welding the use of a low carbon content stainless steel as a filler rod reduces chromium carbide, which improves corrosion resistance [7,12]. However, corrosion resistance can be affected when stainless steel is subjected to cold rolling [13,14]. The friction and compression forces under conditions of dynamic plastic deformation cause the material fibers to stretch while its stress level rises and its hardness increases [15]. Beyond a certain level of deformation different types of defects and even failure can occur. If the process is under control these defects can be avoided, but the relieve of internal stresses requires an annealing treatment [16].

Alike, when materials obtained by cold rolling are welded, the stress state changes due to the effect of heat and the apparition of new stresses during the cooling of the weld, especially if deformation is impeded. These welding stresses depend on the energy applied and the heat transmission conditions during the welding process [17]. Cold rolling and welding are part of various manufacturing processes. So, the combined effect of both in the stresses increment, and its influence in corrosion, can be present in many manufactured products.

The effect of the residual stresses generated during products manufacturing of stainless steel on the stress corrosion cracking susceptibility is presented by [18]. Other works listed below focused on the pitting corrosion, the factors that cause it and their effects: In [19] a summary of the effects of possible factors in the pitting corrosion of metals is given; in [20] cold working was discussed as one factor on the mechanism and rate of pitting corrosion; in [21] the pitting generation caused by applied stress has been studied; in [22] an overview of the critical factors influencing the pitting corrosion of metals is provided; in [23] a method of evaluating strength reduction due to the pitting corrosion is established; in [24] a quantitative analysis of the effect of Type I residual stresses on the occurrence of pitting and stress corrosion is investigated; in [25] the effects of the micro-plasma arc welding technique on the pitting corrosion of different zones of an AISI 316L stainless steel were studied; in [12] the effect of low intensity X-rays ionizing radiation on TIG-welds of AISI 304 stainless steel using AISI 316L as filler rods is analysed.

In this work, a batch of welded samples of AISI 304 stainless steel were subjected to different levels of cold work to change the shape of grains, create residual stresses and damage the surface. The influence of those changes in the pitting corrosion resistance of the welds was evaluated by the immersion of the samples in a $FeCl_3$ solution according to a standardized test and quantified by the pits number [8,26–29]; while deformation levels were measured as the thickness reduction of the metal samples (cold work level). A mathematical relation between the cold work level and the number of pits is proposed for the tested samples.

2. Materials and Experimental Procedures

2.1. Characteristics of Materials Used

The base material of the welded joint (AISI 304), whose chemical composition is given in Table 1, is a non-magnetic weldable austenitic stainless steel with good mechanical characteristics, highly resistant to corrosion, which does not harden in heat treatments and easily deformable by rolling, traction and stamping. The filler metal was low-carbon ER AISI 308L, which reduces the formation of chromium carbide in the grain boundary during welding and is recommended for TIG or MIG (metal inert gas) welding of the AISI 304 steel. The AISI 308L has good corrosion resistance, is non-magnetic, and is principally used in the chemical industry and food applications. Its composition is also shown in Table 1.

Table 1. Chemical composition of AISI 304 and ER AISI 308 L base and filler stainless steels.

Material	%C	%Si	%Mn	%Cr	%Ni	%Mo	%Fe
AISI 304	0.07	1	2	19	11	-	Bal.
ER AISI 308L	0.02	0.38	1.90	19.80	9.8	0.19	Bal.

2.2. Tests Description

2.2.1. Sample Preparation

Welding was carried out on a horizontal plane in an inert argon atmosphere and employing non-consumable tungsten-thorium alloy electrode. The welding parameters were: Gun nozzle exit rate of 11 dm^3/min, current 48 A, applied bias from 10 to 12 V, travel rate of 50 mm/min, torch inclination angle from 70° to 80° and filler rod inclination angle of 15°.

Stainless steel experiments more heat deformation than other carbon steels or steel alloys. So, to avoid significant deformation during the welding process, the plates were fixed until they returned to the ambient temperature. However, the undesired effect of a small residual stress due to the deformation restriction during cooling is expected [30].

The welds were carried out on twelve AISI 304 steel plates measuring 200 mm in length, 100 mm in width, and 1.5 mm thick. Once welded, the plates were cut perpendicularly to the weld bead at 20 mm intervals to obtain 10 samples from each plate; 60 samples in total measuring 100 mm in length, 20 mm in width, and 1.5 mm thick (see Figure 1). The joints were smoothed and polished, removing surface irregularities to obtaining the same thickness as the original plates.

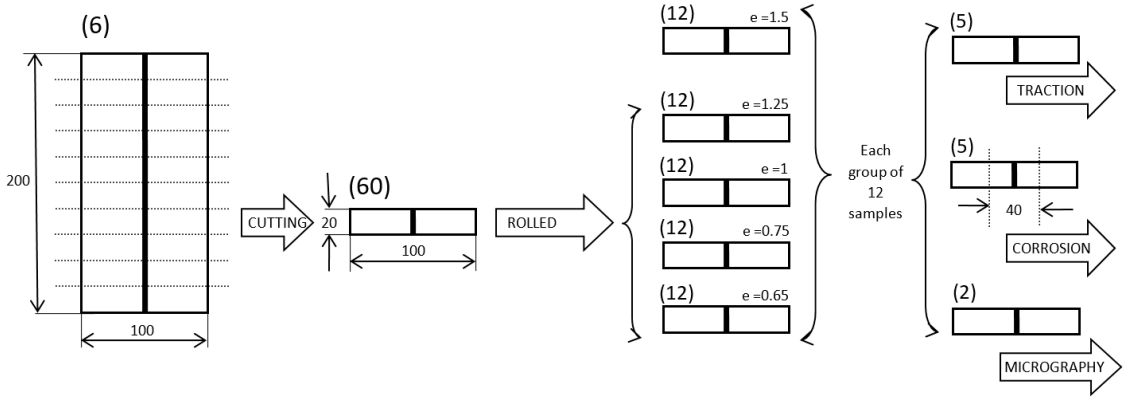

Figure 1. Samples preparation for tests: Number of samples (in brackets), samples dimensions (in mm), and preparation operations and tests to be carried out.

These samples were cold rolled to obtain five different thickness batches: 12 samples of 1.5 mm thick, 12 samples of 1.25 mm thick, 12 samples of 1 mm thick, 12 samples of 0.75 mm thick and

12 samples of 0.65 mm thick. The samples thickness of each batch is expressed as "e" in Figure 1. Those values correspond to cold work percentages of 0%, 17%, 33%, 50% and 57%, respectively.

Subsequently, the samples selected for corrosion tests were cut to 40 mm in length, leaving welds approximately in the center (Figure 1).

2.2.2. Micrographs and Hardness Tests

Two samples from each batch were selected for micrographic tests (Figure 1). One to obtain a surface micrograph and the other for a transversal micrograph. The surface micrographs allowed the study of the changes that take place at the surface and that could lead to a deterioration of the protective passive layer on the stainless plate. The transversal micrographs provide information about the welding microstructure and how the grains are deformed by the rolling process, as the changes in the microstructure driven by plastic deformation could affect the corrosion resistance of the joints.

For the micrographs, the samples were cut as indicated in Figure 2. After cutting, they were polished in two stages: First a grinding with 200 and 500 grain size abrasive paper, followed by a final polishing with 3 µm and 1 µm diamond paste. Finally, the samples were electroetched in a 10% oxalic acid solution.

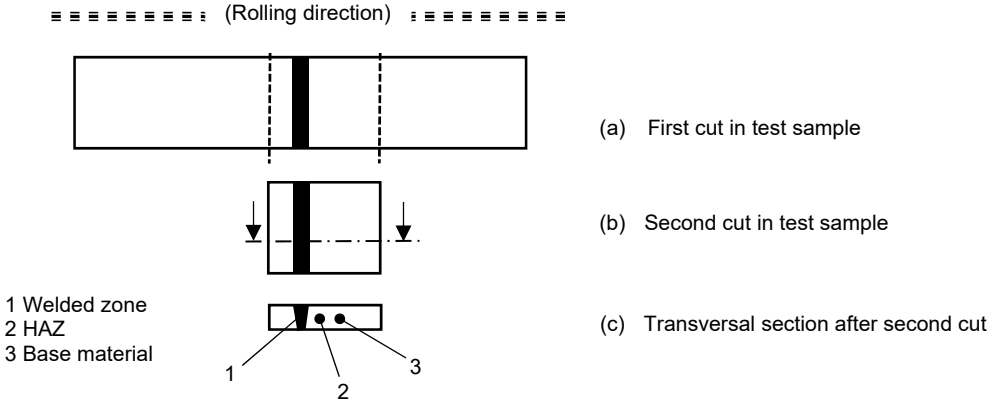

Figure 2. Samples preparation for micrographs and hardness measurement. The dashed triple line represents the rolling direction.

The same samples were used to measure the hardness at the weld bead, the HAZ and the base metal.

The micrographs were made with an Optikam camera (Optika, Ponteranica, Italy) software in a NIKON metallographic microscope Microphot-FX (Nikon, Tokio, Japan). For microhardness testing, a Vickers micro-durometer INNOVATEST 400A (Innovatest, Townley, The Netherlands) with 300 g load was used and 12 s of dwell time.

2.2.3. Tensile Tests

Ultimate and yield strengths were evaluated by tensile tests performed on five samples from each batch (Figure 1) using a 100 kN universal test machine Electrotest MD-2 (Ibertest, Daganzo de Arriba, Spain), at a test speed of 10 mm/min.

2.2.4. Corrosion Tests

Five samples from each batch were selected for corrosion tests (Figure 1). These tests, in accordance with ASTM G48-92 [31], consisted in submerging the samples during 72 h in a 10% mass (0.387 M) solution of iron(III) chloride hexahydrate ($FeCl_3 \cdot 6H_2O$) electrolyte and the subsequent evaluation of the pitting corrosion in the weld and HAZ zones. The $FeCl_3$ provide the Cl^- ions needed to accelerate the corrosion rate as described in the introduction.

3. Results

3.1. Micrographs and Hardnesses

Figures 3–7 show the transversal micrographs performed at the fusion line of welded zones at samples of 1.5 mm to 0.65 mm thick.

In these micrographs the granular deformation due to rolling can be seen at both the weld bead and the HAZ. As the deformation occurred in a cold forming process, the structures changed from dendritic at the weld bead to equiaxial at the HAZs and the base metal. Those structures become clearly elongated as the thickness reduction increases. This difference is progressively reduced as the deformation degree by rolling increases, as can be seen in Figures 3–7.

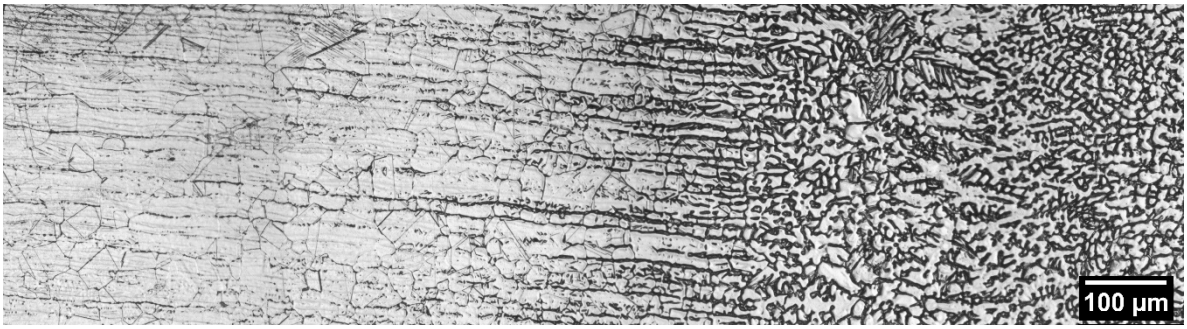

Figure 3. Transversal micrography of the non-rolled sample (1.5 mm thick) at the weld bead (right)/heat affected zone (HAZ) (left) interface.

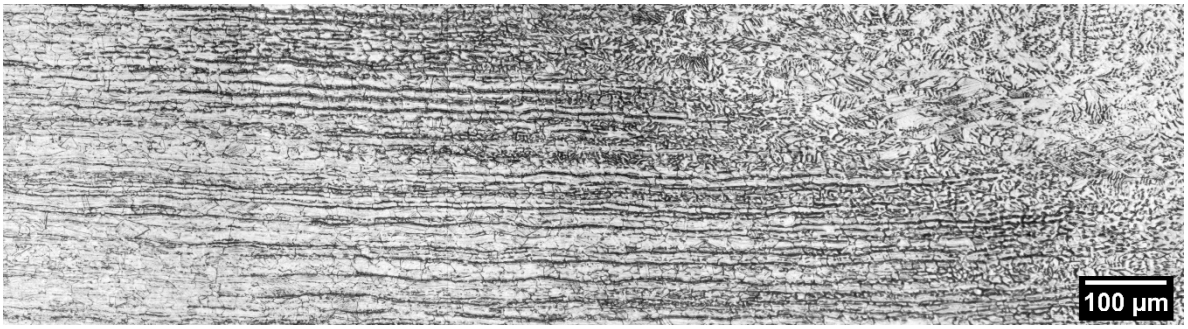

Figure 4. Transversal micrography at the weld bead (right)/HAZ (left) interface after 17% cold rolling.

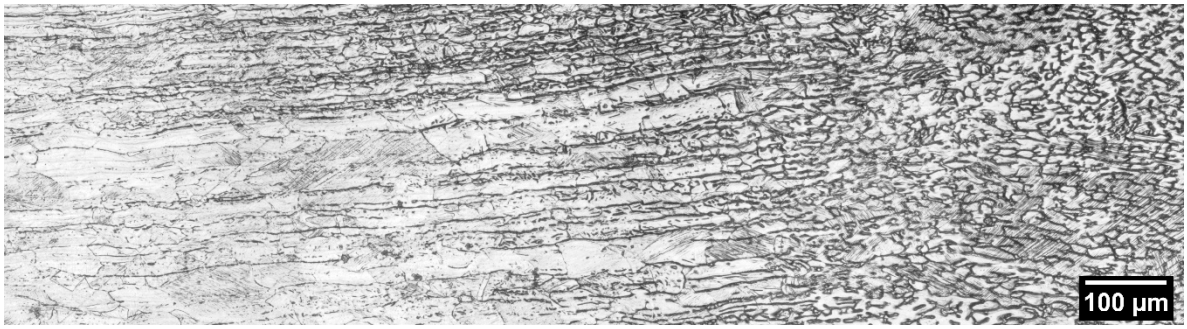

Figure 5. Transversal micrography at the weld bead (right)/HAZ (left) interface after 33% cold rolling.

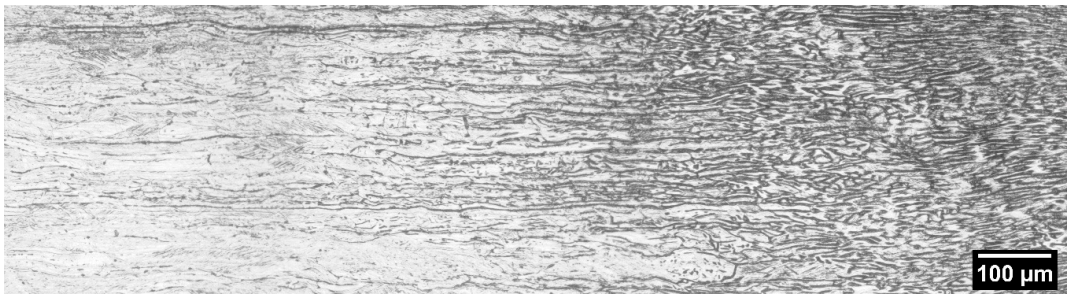

Figure 6. Transversal micrography at the weld bead (right)/HAZ (left) interface after 50% cold rolling.

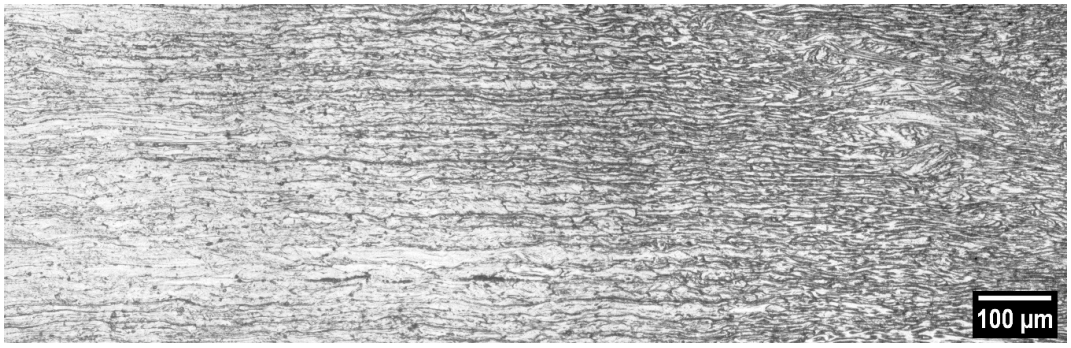

Figure 7. Transversal micrography at the weld bead (right)/HAZ (left) interface after 57% cold rolling.

Figure 8 shows the presence of deformation induced martensite at the samples after deformation. Although the tests were carried out at room temperature and martensite formation is favored by lower temperatures, the cold work level is high enough to compensate for the higher temperatures of the rolling. As stated by [32], the presence of this martensite has a great influence on the performance of the protective layer that covers the deformed samples.

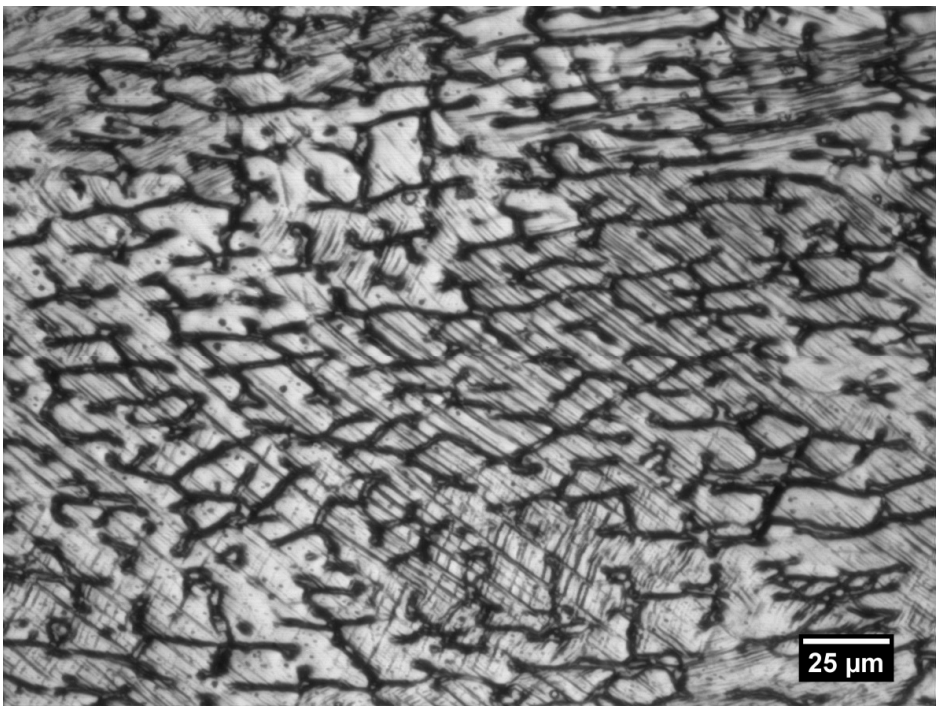

Figure 8. Deformation twins in one of the 33% cold rolled samples. Martensite grows along the deformation twin boundaries.

The high levels of cold work also generated small cracks at the surface of the welded samples (Figure 9). This leads to a decrease in the performance of the protective layer as its continuity is broken and a slight reduction of the mechanical properties when compared to a sample with no cracks.

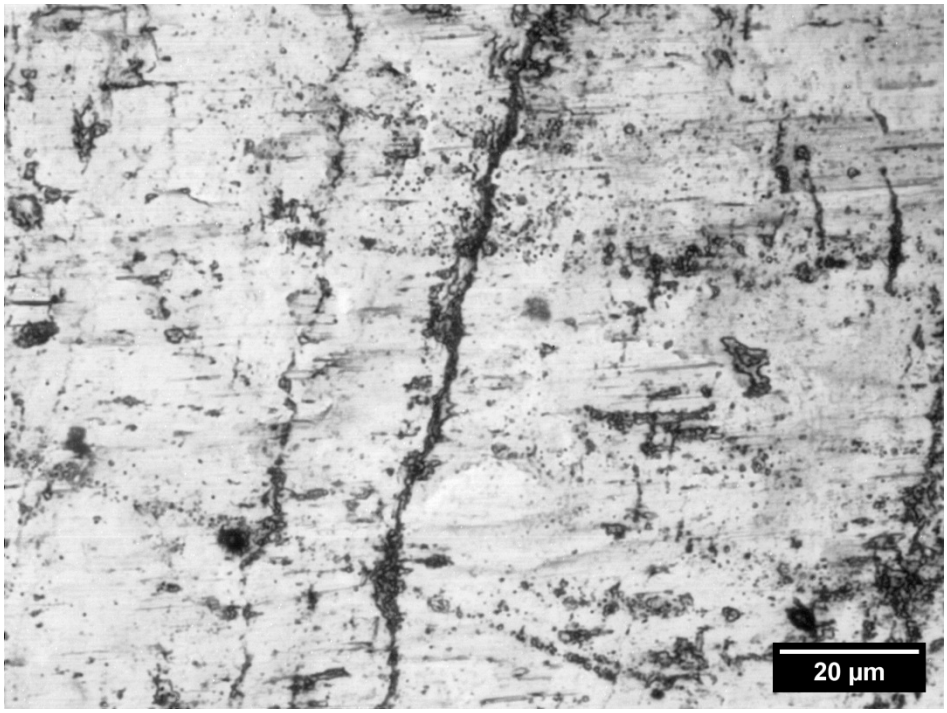

Figure 9. Cracks at the surface after 50% cold rolling.

The results of hardness tests are shown in Table 2, in which the figures given are the average values obtained from the five samples of each batch with their standard deviations. As can be seen, a 50% cold work doubles the hardness of the steel, both in the joint and the base metal, which have similar hardness values in all cases.

Table 2. Hardness test results in the welded, heat affected and base material zones.

Cold Work	Welded Zone (HV)	HAZ (HV)	Base Material (HV)
0%	220 ± 5	221 ± 5	217 ± 2.5
17%	304 ± 1.5	340 ± 2	291 ± 3.7
33%	379 ± 16	435 ± 12	387 ± 7
50%	421 ± 3	470 ± 5.7	416 ± 14
57%	480 ± 3	489 ± 4.5	463 ± 1.3

3.2. Tensile Tests

The results of the tensile tests can be seen in Table 3, in which the values for the yield strength and the tensile strength are the average values obtained from the five samples of each batch, with their standard deviations.

Table 3. Resistance characteristics obtained from tensile tests.

Cold Work	Tensile Strength (MPa)	Yield Strength (MPa)
0%	480 ± 17	180 ± 14
17%	760 ± 20	360 ± 16
33%	800 ± 16	580 ± 15
50%	1170 ± 25	930 ± 20
57%	1200 ± 29	1120 ± 26

3.3. Corrosion Tests

Figure 10 shows an example of the pitting corrosion tests on a cold rolled sample.

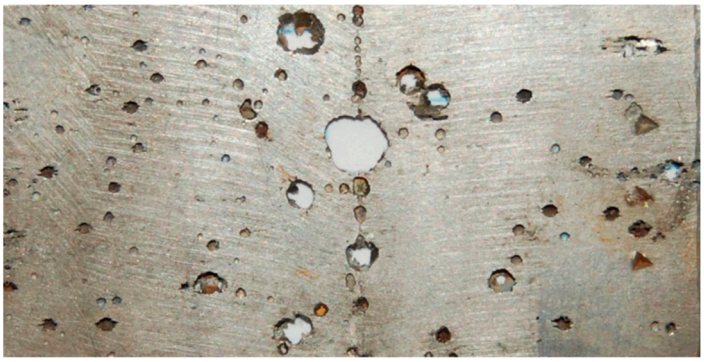

Figure 10. Pitting at the welding and HAZ zones of a 33% cold work sample.

Table 4 gives the average value of the yield strength and the average number of pits. The number of pits was determined in a 20 mm long area of the HAZ (whose limits are equidistant to the weld) using a 50× magnifying glass and the image counting system provided by the software ImageJ.

Table 4. Yield strength and number of pits per m^2.

Cold Work	Yield Strength (MPa)	Pits Number ($10^3/m^2$)
0%	180	175
17%	360	185
33%	580	225
50%	930	320
57%	1120	400

Except for the undeformed samples, all of them presented big pits that perforated the samples.

4. Analysis of Results and Discussion

Figure 11 shows the correlation between the cold work level (percentage of width reduction) and the number of pits (an indicator of the corrosion degree). The following expression, obtained by a least squares fit, models this correlation:

$$y = 165316 + 8343 \cdot e^{0.0585 \cdot x},$$

where:

y = Pits number/m^2
x = Cold work (%)

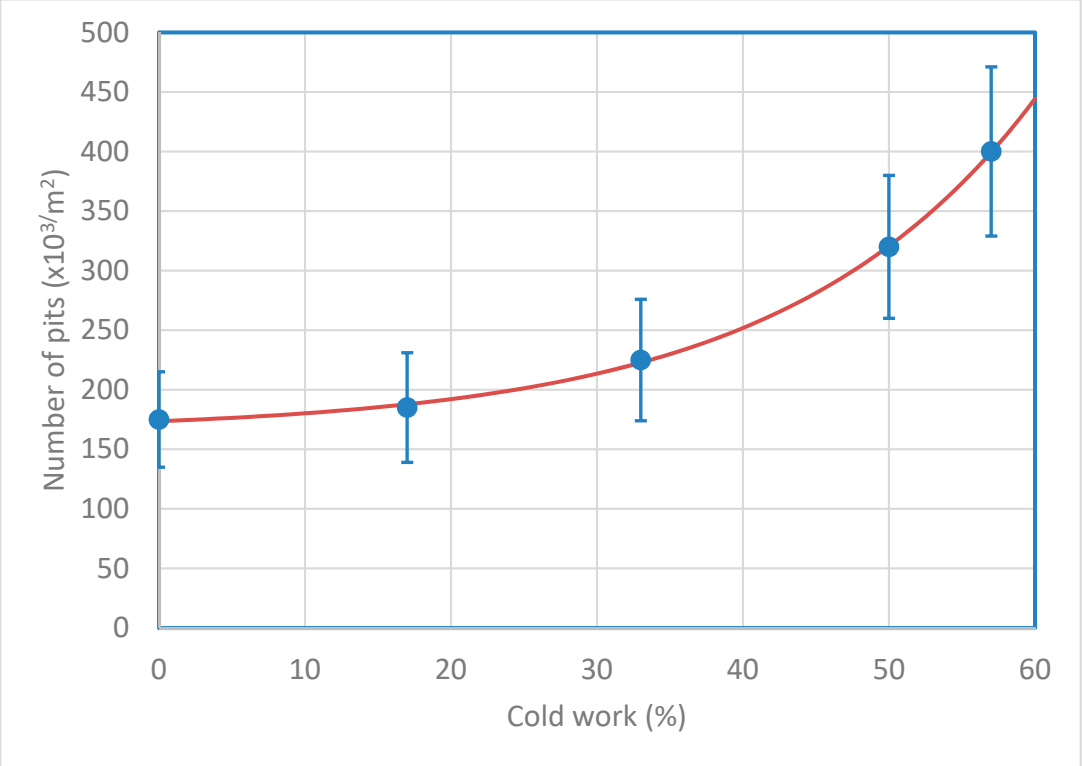

Figure 11. Graphical representation of the correlation between the cold work and number of pits in a 10% mass solution of $FeCl_3 \cdot 6H_2O$.

According to [21], the linear dependence of the pit generation rate on the potential suggests that the pitting process is controlled by an electromechanical breakdown of the passive film. This conclusion could support the correlation found between the cold work level and the number of pits at the present study, that has been represented in Figure 11.

About the result of the corrosion test, we must first consider that the effectiveness of the surface layer of chromium oxide, which acts as a protective agent against corrosion in stainless steels, can be reduced due to the rolling mechanical effects that could lead to a thickness reduction and/or breakage of this protective layer, as evidenced by the presence of small surface cracks in the cold rolled samples. Furthermore, the study carried out in [33] focused on the welding of 304 L austenitic stainless steel by the shielded metal arc welding process using a standard 308 L electrode, shows that, during sensitization, chromium in the matrix precipitates out as carbides and intermetallic compounds on grain boundary, decreasing the corrosion resistance. Similar results are found in [34], and [35] which associates the precipitation of chromium nitride with the reduction of the corrosion resistance of the nitrided layer.

In the AISI 304 stainless steel welding, pitting is concentrated in Cr-depleted regions adjacent to the carbide precipitates [11]. The studies about the effect of microstructural changes in the AISI 304 stainless steel induced by TIG welding, and surely other welding techniques, on the pitting corrosion behavior conclude that the process made the weld metal and HAZ zone more sensitive to the pitting corrosion than the base metal [36]. This work also concludes that high heat-input (and low cooling rate) was likely to induce the segregation of alloying elements and formation of Cr-depleted zones, resulting in decreasing the corrosion resistance [36]. Even more, under [11] study, TIG-welds exhibit lower pitting corrosion resistance than friction and electron beam welds. In fact, austenitic stainless steels are prone to sensitization when subjected to higher temperatures during the manufacturing process. In particular, the study of [27] emphasizes the essential role of temperature-affected variations of the properties of oxide films and their effect on the pitting corrosion in the AISI 304 stainless steel.

The pitting corrosion occurs as a result of a breakdown of the protective passive film on the metal surface [22,37–39] and according to [25], the lowest pitting corrosion resistance behavior is shown in the heat affected zone.

A relevant experimental result, described by [40], is the appearance of the strain-induced martensite, transformed from austenite during the cold working process that can be observed in Figure 4. Which could be related with the appearance of corrosion points, since the formation of micro-pitting occurs preferentially in areas where the tensile residual stresses are the highest [41].

After analyzing the reduction of the anti-corrosion protection in AISI 304 rolled stainless steel welding, it is worth considering how to mitigate the factors that trigger it (chromium concentration decreases in the protective layer and deformation stresses in the material). We have previously commented that the use of a low-carbon filler material reduces chromium carbide formation in the grain boundaries during welding and so, maintains chromium concentration at adequate levels [6,7]. Regarding the deformation stresses reduction, heat treatments are not feasible. As a result of the plate thicknesses considered, stress-reducing heat treatments will cause serious deformations such as unacceptable flatness errors. Another consideration pointed out by [42] is to improve the corrosion resistance of austenitic stainless steels, like AISI 304, through surface finishing treatments, which has been demonstrated beneficial regarding the localized pitting corrosion properties in stainless steels [43]. However, it also must be considered that the residual stress introduced by certain surface finishes affects the corrosion behavior of austenitic stainless steel [13].

Finally, due to the practical impossibility of avoiding the negative effects on corrosion resistance of the manufacture of thin AISI 304 rolled stainless steel welded plates, one alternative would be to select the thickness of the material used according to its expected use conditions, for which the information in Table 4 could be used.

5. Conclusions

Corrosion resistance of AISI 304 rolled stainless steel welding can be altered at both the welded and the HAZ zones due to the effects of cold rolling and the metallurgic transformations and physic-chemical processes that occur during welding, including residual stresses distribution.

The increment of the pitting corrosion in AISI 304 rolled stainless steel welding can be attributed to a combination of factors: The reduction of the anti-corrosion protection, the microstructural changes resulting from the cold rolling process and the internal increased stresses.

Both the chromium concentration decrease, that causes thickness reduction and/or breakage of the chrome oxide protective layer, and the increment of stresses in the samples have been observed in the experimental results. Martensite induced by deformation, transformed from austenite during rolling has also been observed in the experimental results.

All these changes, which promote the local pitting corrosion in the AISI 304 rolled stainless steel weld, are difficult to prevent.

The pitting corrosion degree in AISI 304 cold rolled welds was evaluated in a $FeCl_3$ solution following the ASTM G48-11 standard. The corrosion resistance of the samples was measured using the number of pits and correlated with the deformation level of these samples. The number of pits varied from $175 \cdot 10^3$ pits/m^2 for the undeformed samples to $400 \cdot 10^3$ pits/m^2 for a 57% cold work level.

The exponential expression that correlates cold work levels and pits number, if confirmed, can be useful in the design and material selection for products and facilities including the AISI 304 rolled stainless steel butt-welded, since it provides a simple (not expensive) method to assess the material thickness suitability regarding its corrosion resistance.

Author Contributions: In this investigation, F.-J.C.-C., M.P.-G. and F.S.V. conceived and designed the experiments; F.-J.C.-C., L.S.G. and M.-A.P.-P. performed the experiments; M.P.-G., L.S.G. and F.S.V. analyzed the data; M.-A.P.-P. contributed materials/analysis tools; M.P.-G., L.S.G. and F.S.V. wrote the paper.

Funding: This research received no external funding.

Acknowledgments: The authors deeply thank the Universitat Politècnica de València (Spain), for the support of this research.

Conflicts of Interest: The authors declare no conflict of interest.

References

1. Khatak, H.S.; Raj, B. *Corrosion of Austenitic Stainless Steels Mechanism, Mitigation and Monitoring*; Woodhead Publishing Series in Metals and Surface Engineering; Woodhead Publishing: Delhi, India, 2002; pp. 74–105. ISBN 978-1-85573-613-9.
2. Sathiya, P.; Aravindan, S.; Haq, A. Mechanical and metallurgical properties of friction welded AISI 304 austenitic stainless steel. *Int. J. Adv. Manuf. Technol.* **2005**, *26*, 505–511. [CrossRef]
3. Gong, N.; Wu, H.; Yu, Z.; Niu, G.; Zhang, D. Studying Mechanical Properties and Micro Deformation of Ultrafine-Grained Structures in Austenitic Stainless Steel. *Metals* **2017**, *7*, 188. [CrossRef]
4. Fellinger, J.; Citarella, R.; Giannella, V.; Lepore, M.; Sepe, R.; Czerwinski, M.; Herold, F.; Stadler, R. Overview of fatigue life assessment of baffles in Wendelstein 7-X. *Fusion Eng. Des.* **2018**, *136*, 292–297. [CrossRef]
5. Lv, J.; Liang, T.; Luo, H. Influence of pre-deformation, sensitization and oxidation in high temperature water on corrosion resistance of AISI 304 stainless steel. *Nucl. Eng. Des.* **2016**, *309*, 1–7. [CrossRef]
6. Hsu, C.-H.; Chen, T.-C.; Huang, R.-T.; Tsay, L.-W. Stress Corrosion Cracking Susceptibility of 304L Substrate and 308L Weld Metal Exposed to a Salt Spray. *Materials* **2017**, *10*, 187. [CrossRef] [PubMed]
7. Ramkumar, K.; Arivazhagan, N.; Narayanan, S. Effect of filler materials on the performance of gas tungsten arc welded AISI 304 and Monel 400. *Mater. Des.* **2012**, *40*, 70–79. [CrossRef]
8. Bhandari, J.; Lau, S.; Abbassi, R.; Garaniya, V.; Ojeda, R.; Lisson, D.; Khan, F. Accelerated pitting corrosion test of 304 stainless steel using ASTM G48; Experimental investigation and concomitant challenges. *J. Loss Prev. Process Ind.* **2017**, *47*, 10–21. [CrossRef]
9. Sampaio, J.P.; Carvalho, C.; Cabral, A.V.; Batista, H.; Pereira, J. Effect of temperature on the level of corrosion caused by heavy petroleum on AISI 304 and AISI 444 stainless steel. *Mater. Res.* **2006**, *9*, 137–142.
10. Gooch, T.G. Corrosion Behavior of Welded Stainless Steel. *Weld. Res.* **1996**, *75*, 135s.
11. Madhusudhan Reddy, G.; Mohandas, T.; Sambasiva Rao, A.; Satyanarayana, V.V. Influence of welding processes on microstructure and mechanical properties of dissimilar austenitic-ferritic stainless steel welds. *Mater. Manuf. Process.* **2005**, *20*, 147–173. [CrossRef]
12. Cárcel-Carrasco, F.J.; Pascual-Guillamón, M.; Pérez-Puig, M.A. Effects of X-rays Radiation on AISI 304 Stainless Steel Weldings with AISI 316L Filler Material: A Study of Resistance and Pitting Corrosion Behavior. *Metals* **2016**, *6*, 102. [CrossRef]
13. Takakuwa, O.; Soyama, H. Effect of Residual Stress on the Corrosion Behavior of Austenitic Stainless Steel. *Adv. Chem. Eng. Sci.* **2015**, *5*, 62–71. [CrossRef]
14. Peguet, L.; Malki, B.; Baroux, B. Influence of cold working on the pitting corrosion resistance of stainless steels. *Corros. Sci.* **2007**, *49*, 1933–1948. [CrossRef]
15. Agrawal, A.K.; Singh, A. Limitations on the hardness increase in 316L stainless steel under dynamic plastic deformation. *Mater. Sci. Eng.* **2017**, *687*, 306–312. [CrossRef]
16. Hu, J.; Marciniak, Z.; Duncan, J. *Mechanics of Sheet Metal Forming*; Butterworth-Heinemann: Oxford, UK, 2002; ISBN 0-7506-5300-0.
17. Masubuchi, K.; Blodgett, O.W.; Matsui, S.; Ruud, C.O.; Tsai, C.L. Residual stress and distortion. In *Welding Handbook Welding Science & Technology*, 9th ed.; Jenney, C.L., O'Brien, A., Eds.; American Welding Society: Miami, FL, USA, 2001; Volume 1, pp. 297–357. ISBN 0-87171-657-7.
18. Ghosh, S.; Kain, V.; Rana, V.P.S.; Mittal, V.; Baveja, S.K. Role of residual stresses induced by industrial fabrication on stress corrosion cracking susceptibility of austenitic stainless steel. *Mater. Des.* **2011**, *32*, 3823–3831. [CrossRef]
19. Kolotyrkin, J.A.M. Pitting Corrosion of Metals. *Corrosion* **1963**, *19*, 261–268. [CrossRef]
20. Szklarska-Smialowska, Z. Review of Literature on Pitting Corrosion Published Since 1960. *Corrosion* **1971**, *27*, 223–233. [CrossRef]
21. Shibata, T.; Takeyama, T. Stochastic Theory of Pitting Corrosion. *Corrosion* **1977**, *33*, 243–251. [CrossRef]
22. Frankel, G.S. Pitting Corrosion of Metals. A Review of the Critical Factors. *J. Electrochem. Soc.* **1998**, *145*, 2186–2198. [CrossRef]

23. Nakai, T.; Matsushita, H.; Yamamoto, N. Effect of pitting corrosion on the ultimate strength of steel plates subjected to in-plane compression and bending. *J. Mar. Sci. Technol.* **2006**, *11*, 52–64. [CrossRef]
24. Chen, W.; Van Boven, G.; Rogge, R. The role of residual stress in neutral pH stress corrosion cracking of pipeline steels–Part II: Crack dormancy. *Acta Mater.* **2007**, *55*, 45–53. [CrossRef]
25. Sánchez-Tovar, R.; Montañés, M.T.; García-Antón, J. Effect of the micro-plasma arc welding technique on the microstructure and pitting corrosion of AISI 316L stainless steels in heavy LiBr brines. *Corros. Sci.* **2011**, *53*, 2598–2610. [CrossRef]
26. Pistorius, P.C.; Burstein, G.T. Metastable pitting corrosion of stainless steel and the transition to stability. *Philos. Trans. R. Soc. A Math. Phys. Eng. Sci.* **1992**, *341*, 531–559.
27. Wang, J.-H.; Su, C.C.; Szklarska-Smialowska, Z. Effects of Cl−Concentration and Temperature on Pitting of AISI 304 Stainless Steel. *Corros. Sci.* **1988**, *44*, 732–737. [CrossRef]
28. Pardo, A.; Merino, M.C.; Coy, A.E.; Viejo, F.; Arrabal, R.; Matykina, E. Pitting corrosion behaviour of austenitic stainless steels–Combining effects of Mn and Mo additions. *Corros. Sci.* **2008**, *50*, 1796–1806. [CrossRef]
29. Lin, C.-M.; Tsai, H.-L.; Cheng, C.-D.; Yang, C. Effect of repeated weld-repairs on microstructure, texture, impact properties and corrosion properties of AISI 304L stainless steel. *Eng. Fail. Anal.* **2012**, *21*, 9–20. [CrossRef]
30. Sepe, R.; Laiso, M.; De Luca, A.; Caputo, F. Evaluation of residual stresses in butt welded joint of dissimilar material by FEM. *Key Eng. Mater.* **2017**, *754*, 268–271. [CrossRef]
31. ASTM G48-92. *Standard Test Methods for Pitting and Crevice Corrosion Resistance on Stainless Steels and Related Alloys by Use of Ferric Chloride Solution*; ASTM: West Conshohocken, PA, USA, 2009.
32. He, S.; Jiang, D.; Sun, Z. Effect of deformation-induced martensite on protective performance of passive film on 304 stainless steel. *Int. J. Electrochem. Sci.* **2018**, *13*, 4700–4719. [CrossRef]
33. Unnikrishnan, R.; Idury, K.S.; Ismail, T.P.; Bhadauria, A.; Shekhawat, S.K.; Khatirkar, R.K.; Sapate, S.G. Effect of heat input on the microstructure, residual stresses and corrosion resistance of 304L austenitic stainless steel weldments. *Mater. Charact.* **2014**, *93*, 10–23. [CrossRef]
34. Abe, F. Precipitate design for creep strengthening of 9% Cr tempered martensitic steel for ultra-supercritical power plants. *Sci. Technol. Adv. Mater.* **2008**, *9*, 013002. [CrossRef]
35. Liang, W. Surface modification of AISI 304 austenitic stainless steel by plasma nitriding. *Appl. Surf. Sci.* **2003**, *211*, 308–314. [CrossRef]
36. Lu, B.T.; Chen, Z.K.; Luo, J.L.; Patchett, B.M.; Xu, Z.H. Pitting and stress corrosion cracking behavior in welded austenitic stainless steel. *Electrochim. Acta* **2005**, *50*, 1391–1403. [CrossRef]
37. Strehblow, H.H. Breakdown of passivity and localized corrosion: Theoretical concepts and fundamental experimental results. *Mater. Corros.* **1984**, *35*, 437–448. [CrossRef]
38. Marcus, P.; Maurice, V.; Strehblow, H.H. Localized corrosion (pitting): A model of passivity breakdown including the role of the oxide layer nanostructure. *Corros. Sci.* **2008**, *50*, 2698–2704. [CrossRef]
39. Soltis, J. Passivity breakdown, pit initiation and propagation of pits in metallic materials–Review. *Corros. Sci.* **2015**, *90*, 5–22. [CrossRef]
40. Guan, K.; Zhang, X.; Gu, X.; Cai, L.; Xu, H.; Wang, Z. Failure of 304 stainless bellows expansion joint. *Eng. Fail. Anal.* **2005**, *12*, 387–399. [CrossRef]
41. Van Boven, G.; Chen, W.; Rogge, R. The role of residual stress in neutral Ph stress corrosion cracking of pipeline steels. Part I: Pitting and cracking occurrence. *Acta Mater.* **2007**, *55*, 29–42. [CrossRef]
42. Ben Rhouma, A.; Sidhom, H.; Braham, C.; Lédion, J.; Fitzpatrick, M.E. Effects of surface preparation on pitting resistance, residual stress, and stress corrosion cracking in austenitic stainless steels. *J. Mater. Eng. Perform.* **2001**, *10*, 507–514. [CrossRef]
43. Peyre, P.; Scherpereel, X.; Berthe, L.; Carboni, C.; Fabbro, R.; Béranger, G.; Lemaitre, C. Surface modifications induced in 316L steel by laser peening and shot-peening. Influence on pitting corrosion resistance. *Mater. Sci. Eng. A* **2000**, *280*, 294–302. [CrossRef]